Energy, Mines and Resources Canada | Énergie, Mines et Ressources Canada

CANMET

Canada Centre for Mineral and Energy Technology | Centre canadien de la technologie des minéraux et de l'énergie

ELECTROCHEMICAL CELL ELECTRODE MATERIALS AND PERFORMANCE

J.D. Canaday, A.K. Kuriakose, T.A. Wheat, and A. Ahmad
Ceramic Section
Mineral Processing Laboratory

December 1986

Project: 30.29.01
Advanced Ceramic Materials

This document is an unedited interim report prepared primarily for discussion and internal reviewing purposes. It does not represent a final expression of the opinion of the Canada Centre for Mineral and Energy Technology (CANMET)

Ce document est un rapport préliminaire non-révisé et rédigé [illegible] pour fin de discussion et de documentation interne. Il ne représente nulle[illegible]ion définitive de l'opinion du Centre canadien de la technologie des minéraux et de l'énergie (CANMET)

21 pp

MINERAL RESEARCH PROGRAM
MINERAL SCIENCES LABORATORIES
DIVISION REPORT MSL 86-156 (IR)

Crown Copyrights Reserved

MICROMEDIA

ELECTRICAL CELL ELECTRODE MATERIALS AND PERFORMANCE

by

J.D. Canaday, A.K. Kuriakose

T.A. Wheat and A. Ahmad

ABSTRACT

An investigation of several electrode materials for use with solid protonic electrolytes has been conducted. It was found that the most suitable composition is a commercial platinum paste.

Electrical measurements of a fuel cell containing a Nasicon electrolyte and platinum electrodes are also discussed. Cell performance data indicate that a maximum current density of 0.3 mA cm^{-2} was obtained. Polarization measurements showed that both the anode and the cathode become polarized during cell discharge; the mechanism is believed to be an activation process. This mechanism occuring at the electrodes and the IR loss of the electrolyte are shown to contribute in approximately equal amounts to the reduction of the fuel cell voltage.

Keywords: electrodes, solid electrolytes, fuel cells, polarization

LES MATÉRIAUX POUR ÉLECTRODES DE PILES ÉLECTRIQUES ET LEUR RENDEMENT

par

J.D. Canaday, A.K. Kuriakose,

T.A. Wheat et A. Ahmad

RÉSUMÉ

Une recherche touchant plusieurs matériaux d'électrodes utilisés avec des électrolytes protoniques solides a été effectuée. Il a été découvert que la composition la plus appropriée est la pâte de platine commerciale.

Les mesures électriques d'une pile à combustible contenant un électrolyte Nasicon et des électrodes de platine sont aussi discutées. Les données sur le rendement de la pile indiquent qu'une densité maximale de courant de 0,3 mA cm^{-2} a été obtenue. Les mesures de polarisation ont montré que l'anode et la cathode deviennent polarisées pendant le déchargement de la pile; il semblerait que la cause de ce phénomène serait due à un processus d'activation. Ce mécanisme qui survient aux électrodes et aussi la chute ohmique de l'électrolyte ont montré qu'ils contribuaient de façon approximativement égale à la réduction du voltage de la pile à combustible.

INTRODUCTION

The CANMET Fuel Cell Program was initiated in 1980 with the purpose of utilizing ceramic materials as the electrolytes. These materials included β"-alumina and Nasicon compositions [1,2]. An ion exchange process [3] has made it possible to replace the mobile cationic species of these electrolytes with hydronium. This result has led to the utilization of the solid protonic materials as the electrolyte in a number of hydrogen devices including sensor, pump, and fuel cell applications.

Under this Program, work on electrode development began with an analysis of various materials which could be used at the anode and cathode [4]. Selection criteria included chemical and mechanical stability, electrochemical activity, and cost. Materials identified as anode candidates were Pt, Au, Ni, and $LaNi_5$, while potential cathode materials were found to be Pt, Au, and $LaCoO_3$ or a similar perovskite.

Next, the morphological characteristics of the electrodes were considered [5]. Parameters such as porosity, permeability, surface area, and three-phase line were identified as factors in the operation of an electrochemical cell. A contract was issued to the Ontario Research Foundation [6] for the examination of those properties. Techniques utilized in this investigation have included SEM/image analysis, gas adsorption, mercury porosimetry, profilometry, permeability, and fractal analysis. The Technical University of Nova Scotia is attempting to produce perovskite electrodes for the cells by the plasma spray method [7].

Gas phase relations for protonic electrolyte cells were considered [8]. The effects of static and dynamic gases were assessed, and it was found that the rate of molecular incidence at the electrode surface from gas flow was insignificant relative to that caused by thermal motion during laminar flow. Thus, disk or tubular cell geometry will not be affected by gas flow considerations.

A polarization model for protonic solid electrolyte fuel cells has also been developed [9]. It was determined that concentration polarization, due to the reactant gas species, can be eliminated by controlling the electrode morphological parameters of porosity and thickness. Peak power densities were calculated for various electrolyte thicknesses and conductivities.

After the minimization of concentration polarization and ohmic loss, activation polarization was seen to be the rate-limiting process of the cell.

A number of electrochemical devices, based on solid protonic electrolytes, have been constructed and evaluated [10]. A hydrogen sensor was compared experimentally with its Nernstian characteristics and was found to operate effectively. Current-voltage data were used to determine the cell performance of a hydrogen pump. A current density of 15 mA/cm^2 was measured at an applied voltage of 30V.

Theoretical Considerations

The operating voltage of an electrochemical cell is given [11] by:

$$V_{cell} = V_{eg} \pm V_p \qquad (1)$$

where V_{eg} and V_p are the equilibrium and polarization terms. The positive sign applies when the cell is driven externally in the case of an electrolyzer, and the negative sign holds for an internally driven cell such as a fuel cell. Figure 1 shows the schematic structure of a solid electrolyte cell. Polarization processes are caused by activation, V_{act}, and concentration, V_{conc}, mechanisms at the electrodes and by the ohmic loss, IR_b, of the bulk electrolyte. These processes combine to form a total cell polarizaiton

$$V_p = V_{act} + V_{conc} + IR_b \qquad (2)$$

Electrodes with a 10% porosity deposited on a solid electrolyte at a thickness of 10μm and exposed to hydrogen and oxygen have been shown [8] to result in negligible reactant-gas concentration polarization. Thus, from Equations (1) and (2), the cell voltage in this case is

$$V_{cell} = V_{eg} - V_{act} - IR_b \qquad (3)$$

If the electrode activation polarization is negligible, then the cell voltage is reduced by only the ohmic loss of the bulk electrolyte according to the relation

$$V_{cell} = V_{eg} - IR_b \tag{4}$$

The polarization processes, for the cell as a whole, can be examined by the two-probe method in which current-voltage characteristics are measured from anode to cathode with the entire ohmic contributions of the electrolyte included in the measurement. The anode and cathode effects are not separated, but the total cell overpotential can be determined by subtracting the electrolyte loss.

When it is necessary to distinguish the anodic and cathodic polarization phenomena, a third electrode, the reference electrode, is connected to the electrolyte. The equivalent circuit and the experimental configuration for this three-probe method are shown in Figure 2. Operated as a fuel cell, the anode is negative, while the cathode is positive. Thus, the cell voltage is

$$V_{cell} = V_c - V_a \tag{5}$$

Similarly, for the open-circuit equilibrium condition, the e.m.f. terms are given by

$$V_{eg} = V_{eq,c} - V_{eg,a} \tag{6}$$

Defining the activation polarization (or overpotential) to be positive at each working electrode gives from Equation (3)

$$V_{act} = V_{cell} - V_{eg} - IR_b \tag{7}$$

The total activation polarization for the cell is the sum of the contributions from the anode and the cathode

$$V_{act} = V_{act,a} + V_{act,c} \tag{8}$$

where the current-voltage relationship at each electrode is given by the Butler-Volmer equation

$$J = J_{o,i}[\exp(\beta_i FV_{act,i}/RT) - \exp(-1-\beta_i)FV_{act,i}/RT)] \tag{9}$$

in which the current density, is J=I/A, and A is the cross-sectional area of the electrochemically active interface. The subscript i, indicates that the measurement is made at either the anode or at the cathode. The term, β, is the symmetry factor [11] for single-step electron processes while F is Faraday's constant. the gas constant and temperature are represented by R and T. At large overpotential, Equation (9) reduces to the Tafel form

$$J=J_{o,i}\exp(\beta_i F\, V_{act,i}/RT) \tag{10}$$

while at low overpotentials, expansion of the exponential terms gives the linear or "ohmic" relation

$$R_f = \frac{V_{act,i}}{J} = \frac{RT}{FJ_{o,i}} \tag{11}$$

where the Faradaic resistance, R_F, is found from the slope of the over potential/current-density plot.

The introduction of a reference electrode into the cell, permits the separation of anodic and cathodic polarization effects. This electrode also acts as a voltage divider in which the resistance of the bulk electrolyte, R_b, is partitioned into two components

$$R_b = R_{u,a} + R_{u,c} \tag{12}$$

where the terms $R_{u,a}$ and $R_{u,c}$ are measured in series with the over-potentials at the anode and cathode. The subscript, u, indicates that these resistive effects are uncompensated and that corrections to the measured anodic and cathodic voltages are necessary in order to determine the over-potential at these electrodes.

Combining Equations (5), (6), (7), (8), and (12) gives

$$V_c-V_a = (V_{eq,c} - V_{eq,a}) - (V_{act,a} + V_{act,c}) - A(JR_{u,a} + JR_{u,c}) \tag{13}$$

Separation of the anodic and cathodic terms results in the relations

$$V_a = V_{eq,a} + (V_{act,a} + AJR_{u,a}) \tag{14}$$

and

$$V_c = V_{eq,c} - (V_{act,c} + AJR_{u,c}) \tag{15}$$

at low overpotentials, substitution of Equation (11) into Equations (14) and (15) gives

$$V_a = V_{eq,a} + AJ(R_{F,a} + R_{u,a}) \tag{16}$$

and

$$V_c = V_{eq,c} - AJ(R_{F,a} + R_{u,a}) \tag{17}$$

RESULTS AND DISCUSSION

Electrode Materials

As part of the project to develop electrodes for electrochemical devices, various compositions were prepared and analyzed.

Platinum Paste

Engelhard A-4338 platinum paste was developed for use as electrodes on ZrO_2. The paste was applied to the solid electrolyte with a Q-tip or a paint brush and allowed to dry in air at room temperature. Although the recommended curing temperature is 800°C, it was found that a reasonably complete cure could be obtained by curing the paste at 100°C in a hydrogen atmosphere for one hour. Figure 3(a) shows that the cured platinum is porous with an average pore size of about 1 μm. Stylus measurements indicated that the film is nonuniform with thichnesses ranging from 10-50 μm. Two-probe measurements determined the resistance to be 5-10 ohms.

Another platinum paste, Engelhard A-3380, was also evaluated. This material shown in Figure 3(b) was applied and cured in the same manner as

Englehard A-4338. The resistance of the A-3380 was found to be much higher (≈ 1M ohm) than that of A-4338 electrodes. This result can be explained by the microstructural properties of the two materials. The A-4338 exhibited a network of interconnected particles with a size of ≈ 1 μ. The A-3380 was composed of isolated flat particles with a much larger size and a corresponding high electrical resistance.

Platinum Paste/Graphite

Engelhard platinum No. 4338 was diluted in butyl acetate and applied to the electrolyte. A cure at 80°C in air resulted in a resistance of 20 ohms. Acheson graphite was sprayed on the platinum, and a resistance of 50 ohms was measured.

SPI Carbon Paste/Platinum Powder

A mixture containing 25 mg of SPI carbon paste and 5 mg of Johnson-Matthey platinum powder was applied to glass and Nasicon hydronium substrates. After drying for one hour, the resistance of the electrodes on both substrates was 50 K-ohms. Following a drying period of 24 hours, the resistance decreased to 10 K-ohms, and after a heat treatment at 110°C for one hour, the final resistance was 1 K-ohm.

Nickel Cobaltate

Nickel cobaltate, ($NiCo_2O_4$), electrodes, have been investigated for use with solid protonic electrolytes [12]. The electrodes were prepared from 0.29 g of nickel nitrate, 0.29 g of cobalt nitrate, and 10 cc. water. This slurry was brushed on glass and α-Al_2O_3 samples. Four successive layers were formed and each coating was dried at 100°C and cured at 300°C for one hour. The resistances of the electrode on the glass substrate were 100 K-ohms, 4 K-ohms, 2 K-ohms, and 1 K-ohm. On the α-Al_2O_3 substrates, the resistances were 0.4 M-ohms, 13 K-ohms, 20 K-ohms, and 15 K-ohms.

Cuprous Oxide

The solid protonic electrolyte dodecamolybdophosphoric acid has been studied [13] with cuprous copper acetate oxide, Cu_2O, as electrodes. The cuprous oxide was prepared by reducing [$Cu(CH_3COO)_2$] with hydrazine and

80°C. Maximum current densities under fuel cell discharge of ≈50 mA cm^{-2} were obtained. These values were only a factor of two lower than those obtained using platinum electrodes.

In the present study, cuprous oxide was prepared by dissolving Cu_2O powder in 1 N acetic acid. This solution was brushed on an α-Al_2O_3 substrate and dried in air. The sample was then cured in a hydrogen atmosphere for one hour at 200 °C. The electrode resistance was found to be ≈ 0.5 M-ohms.

Chloroplatinic Acid

A 10% aqueous solution of chloroplatinic acid, H_2PtCl_6 was applied to a Nasicon sample and the electrode was cured at 120°C for one hour in a hydrogen atmosphere. The colour of the electrode following this treatment was black indicating a reduction to elemental platinum. However, two-probe measurements indicated that the resistance of this material was approximately 1 M-ohm. An additional layer of the solution reduced the resistance by a factor of about two.

The resistances of the various electrode compositions are shown in Table 1 and the compositions are ranked in order of increasing resistance. From this evaluation, it is evident that the only suitable electrode materials is the Engelhard A-4338 platinum paste. This composition has been chosen for the electrodes in all of the electrochemical devices developed to date.

It is possible that a very thin and highly resistive electrode will result in suitable performance when used in conjunction with a low resistivity layer. The thin layer would serve as the electrocatalytically active region at the electrode/electrolyte interface, while the thicker layer would be used as a high-conductivity current collector.

Table 1 - Comparison of Electrode Resistance

Electrode Composition	Resistance (ohms)
Platinum Paste Engelhard A-4338	5-10
Platinum Paste Engelhard A-4338 and Graphite	20-50
SPI Carbon Paste and Platinum Powder	1×10^3
Nickel Cobaltate	1×10^4
Cuprous Oxide	5×10^5
Platinum Paste Engelhard A-3380	1×10^6
Platinum deposit from Chloroplatinic Acid	1×10^6

EXPERIMENTAL METHODS

Electronic Measurements

The circuit for measuring fuel cell performance and electrode polarization characteristics is shown in Figure 4. The reference electrode which is connected with silver epoxy to the side of the electrolyte allows for the separation of the anode and cathode effects. However, the reference electrode also acts as a voltage divider of the potential drop across the electrolyte as shown in Figure 1. Thus, the anode and cathode measurements, V_a and V_c, contain uncompensated electrolyte resistances $R_{u,a}$ and

$R_{u,c}$. The sum of these terms is the bulk electrolyte resistance, R_b, as given by Equation (12). In the present experiment, it was not possible to separate the uncompensated resistances from the activation polarization effects, $V_{act,a}$ and $V_{act,c}$. Separation of these components can be achieved by potentiostatic IR compensation or by the current-interrupt technique [11] and will be the subject of future studies.

Cell Performance and Electrode Polarization

Figure 5 shows the fuel cell performance (or discharge) characteristics for a temperature of 110°C. The anode and cathode gases were hydrogen and air at a pressure of one atmosphere. Curve A represents the discharge of a cell in which only ohmic loss of the electrolyte occurs. This relation was calculated from Equation (4) where the bulk resistance of the electrolyte, R_b, was measured with an impedance bridge at a frequency of 1 KHz and was found to be 800 ohms. Curve B is the experimentally measured two-probe discharge of the cell. Thus, by comparing these two curves, it is apparent that polarization effects in excess of that due to the electrolyte loss occur. It can be assumed that under these conditions [9] concentration polarization is negligible at both electrodes. Therefore, the observed polarization effects are due to the electrolyte loss and to activation polarization. A maximum current density of approximately 0.3 mA cm^{-2} was measured. At one half of this value it can be seen that the electrolyte and electrode loss are about the same in magnitude. Thus, electrode polarization and the ohmic loss of the electrolyte contribute in approximately equal proportions to the overall fuel cell discharge.

In Figure 6, the anodic and cathodic polarization effects are shown. These measurements were obtained by connecting a reference electrode to the edge of the electrolyte disk. As discussed previously, this electrode, in addition to separating the anodic and cathodic over potential, also divides the bulk electrolyte resistance into components which are measured at each electrode. Analytically, these effects are given by Equations (14) and (15) or at low over potentials by Equations (16) and (17). These measurements contain contributions from the electrolyte and the electrode. Separation of these effects requires a current-interrupt technique which will be developed in conjunction with a contractural study [14]. It can be observed that polarization occurs at both electrodes with a larger overpotential at the cathode.

CONCLUSIONS

The electrode compositions evaluated in this study, most of which have been utilized in similar solid electrolyte cells, were found to have a very high electronic resistance. The exception to this result was obtained with Engelhard A-4338 platinum paste. The porosity of this material will eliminate concentration polarization due to reactant gas species if the thickness is ≈ 10 μm.

This platinum composition was also evaluated electrically. Two-probe measurements resulted in a maximum current density of 0.3 $mAcm^{-2}$ when the device was operated as a fuel cell. Activation polarization of the electrodes and ohmic loss of the electrolyte were found to contribute in nearly equal amounts to the cell discharge. Three-probe results illustrated that activation polarization occurs at both the anode and the cathode. The use of the current-interrupt method will allow the ohmic losses of the electrolyte to be separated from the activation polarization of each electrode.

Previous studies have shown that Nasicon and beta-alumina electrolytes, when used with platinum paste electrodes, can be operated as a hydrogen sensor and as a hydrogen pump. In order for these components to be effectively utilized in the fuel cell configuration, reductions in electrode activation polarization and electrolyte ohmic loss must be achieved.

REFERENCES

1. Kuriakose, A.K., Wheat T.A., Ahmad A., Canaday J.D., "Synthesis and sintering of sodium-potassium beta/beta" - alumina; Division Report ERP/MSL 85-26 (OP); CANMET, Energy, Mines and Resources Canada, 1985.

2. Kuriakose A.K., Wheat T.A., Ahmad A., DiRocco J., " Synthesis, sintering and microstructure of Nasicons", J. Amer. Ceramic. Soc., 67:179, 1984.

3. Kuriakose, A.K., Wheat T.A., Ahmad A., Canaday J.D., "A new method for the fabrication of polycrystalline hydrogen-conducting solid electrolytes", Division Report ERP/MSL 85-149 (IR); CANMET, Energy, Mines and Resources Canada, 1985.

4. Canaday J.D., Kuriakose A.K., Ahmad A., Wheat T.A., "Electrode materials for protonically conducting solid electrolyte fuel cells", Division Report ERP/MSL 83-120 (IR); CANMET, Energy, Mines and Resources, Canada, 1983.

5. Canaday J.D., Kuriakose A.K., Ahmad A., Wheat T.A., " Electrodes for solid-state electrolyte fuel cells - electrode morphology", Division Report ERP/MSL 83-134 (IR); CANMET, Energy, Mines and Resources, Canada, 1983.

6. DSS File 03SQ.23440-4-9223; "Characterization of thin films used as electrodes in electrochemical devices", Ontario Research Foundation.

7. DSS File 14SQ.23440-5-9212; "Plasma spray of perovskite material for electrochemical cell electrodes", Technical University of Nova Scotia.

8. Canaday J.D., Wheat T.A., Ahmad A., Kuriakose A.K., "Gas phase relations for protonic solid-electrolyte fuel cells", accepted for publication, J. Apl. Electrochem., 1986.

9. Canaday J.D., Wheat T.A., Ahmad A., Kuriakose A.K., "A polarization model for protonic solid-electrolyte fuel cells", accepted for publication, Intl. J. Hydrogen Energy, 1986.

10. Canaday J.D., Kuriakose A.K., Ahmad A., Wheat T.A., "Device applications of hydrogen-conducting solid electrolytes", accepted for publication J. Can. Ceramic Soc., 1986.

11. Canaday J.D., Kuriakose A.K., Wheat T.A., Ahmad A., "An elelctrochemical analysis of solid electrolyte/electrode systems"., CANMET Report CM 86-8E, 1986.

12. Bell M.F. and Sayer M., "Development of electrodes for solid electrolytes"; DSS File 21ST.23440-4-9204; 1986.

13. Nakamura O., Adachi M., Kawai M., Nakahara F., Ogins I., "Copper oxide as oxygen electrode catalyst in a solid electrolyte fuel cell", Mat. Res. Bull. 20:293; 1985.

14. DSS File 04SQ.23440-5-9144; "Analytical investigation of protonic solid electrolyte/electrode polarization mechanisms", The Electrofuel Manufacturing Co.

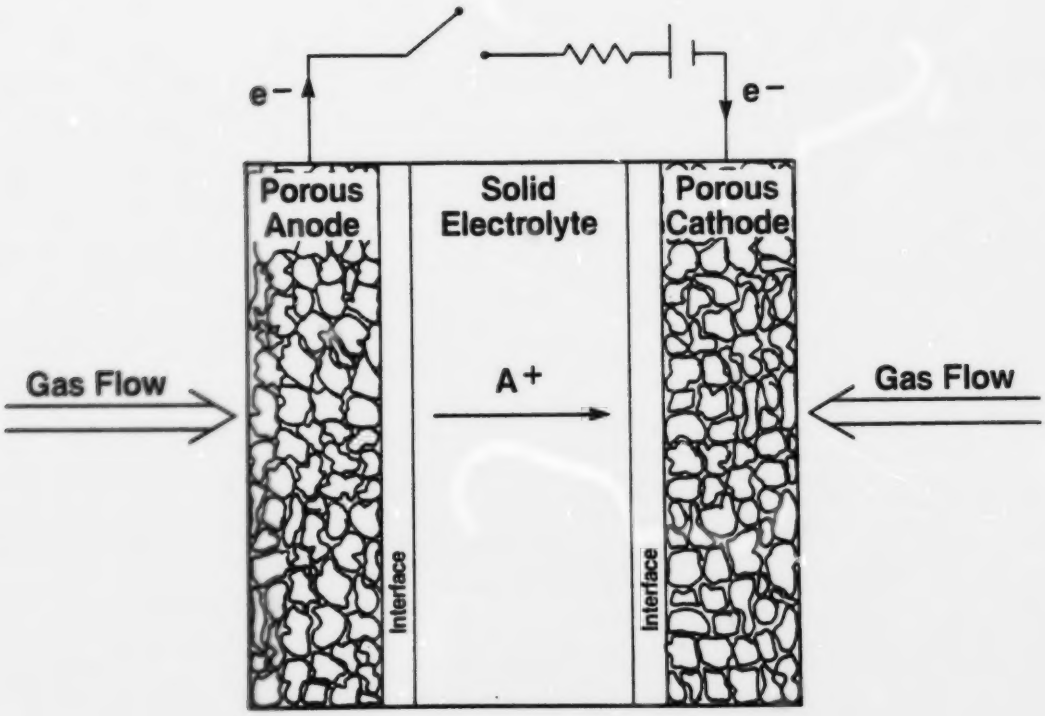

Fig. 1. Structure of a protonically conducting solid electrolyte cell.

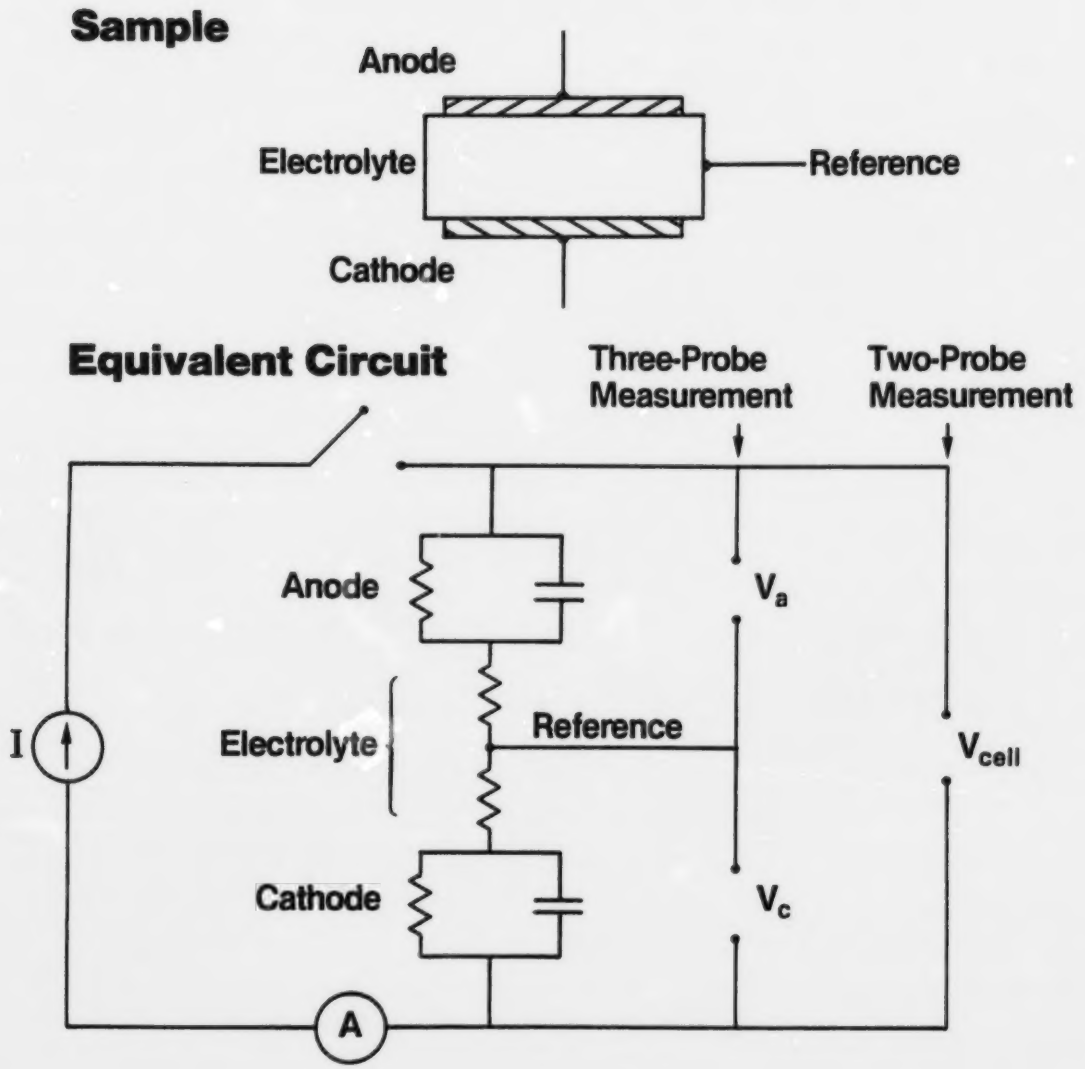

Fig. 2. Sample configuration and equivalent circuit of a solid electrolyte cell.

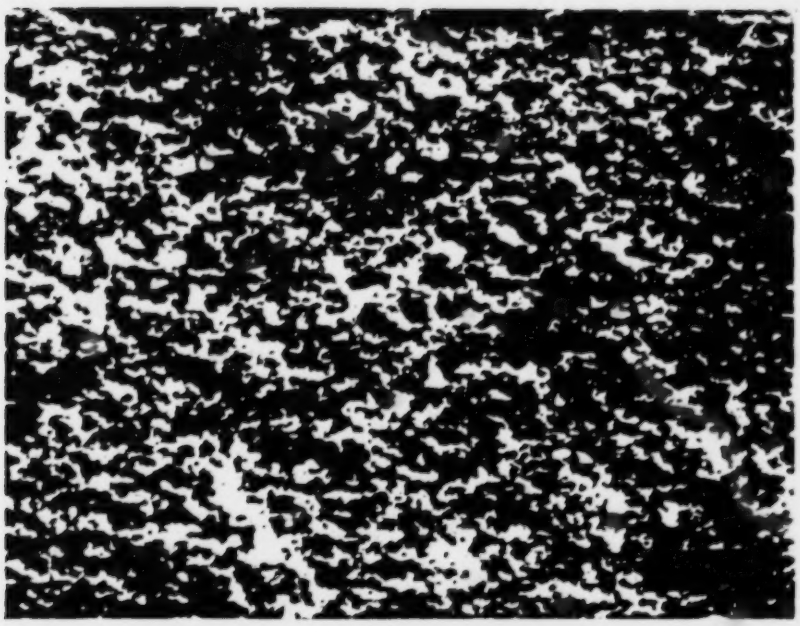

(a)
Engelhard A-4338 Platinum Paste

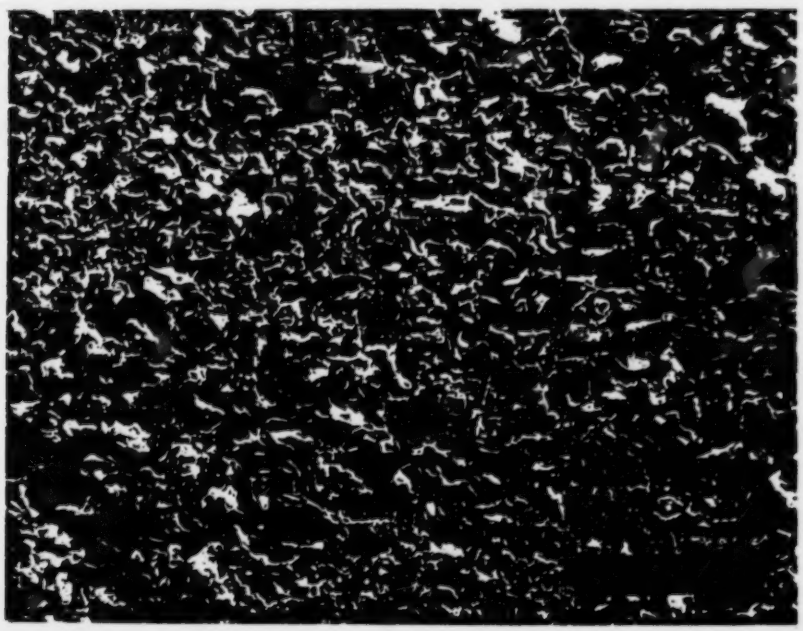

(b)
Engelhard A-3380 Platinum Paste

Fig. 3. Electrode Microstructures.

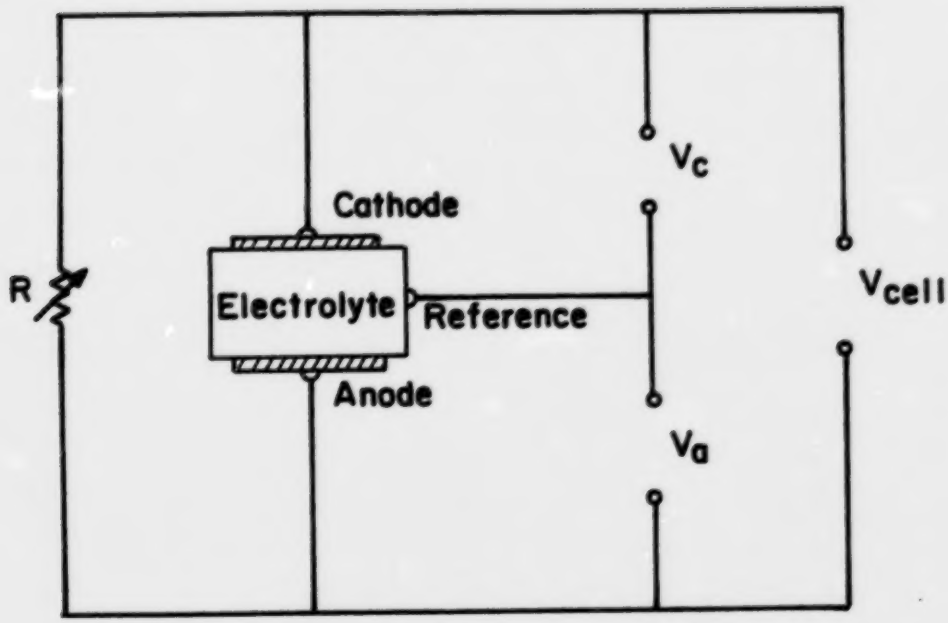

Fig. 4. Experimental circuit for fuel cell discharge.

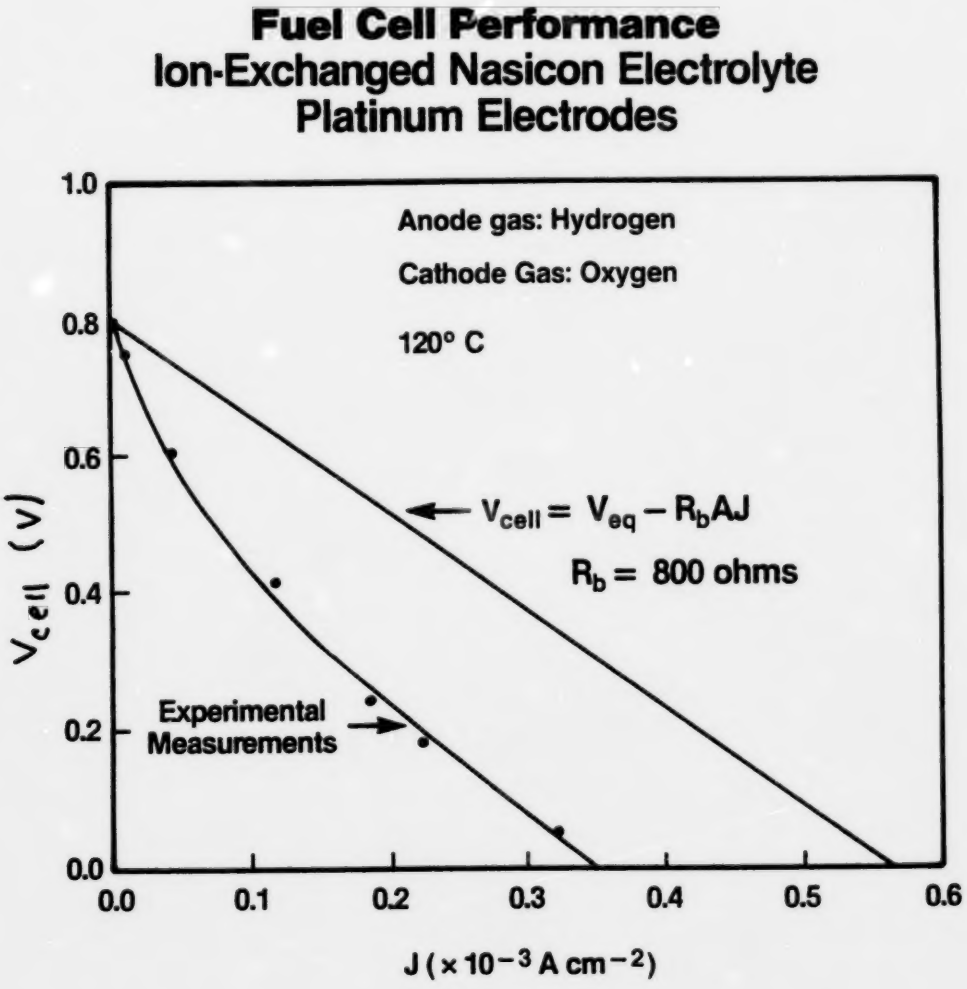

Fig. 5. Fuel cell discharge characteristics.

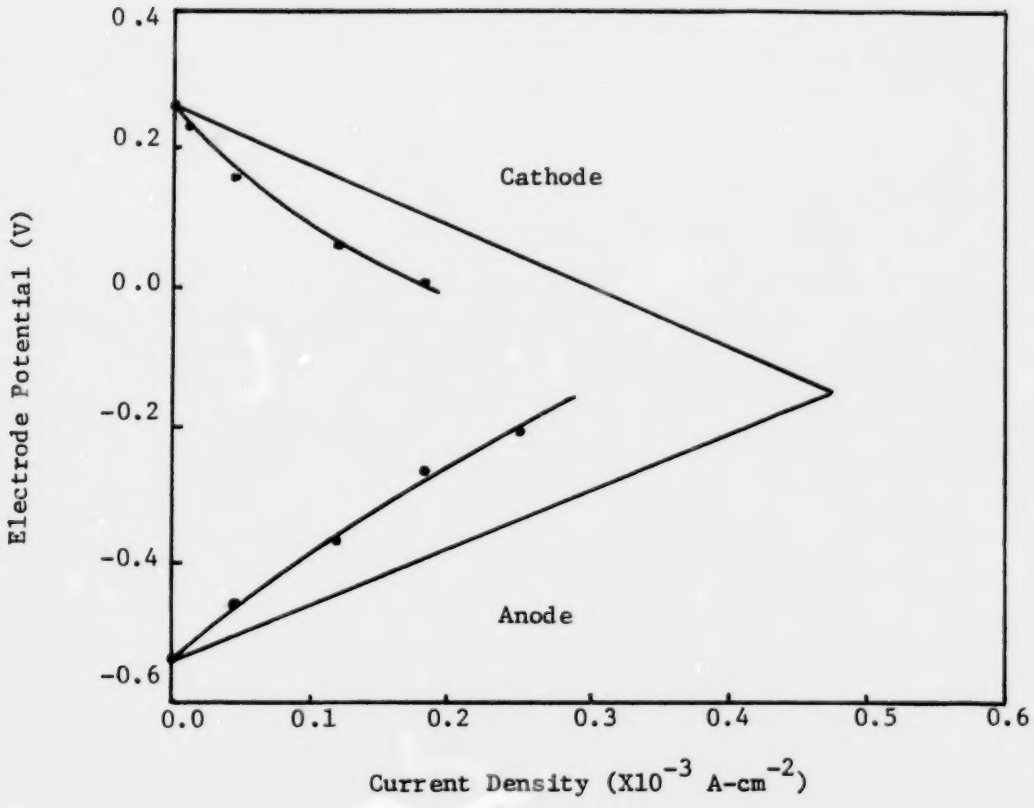

Fig. 6. Fuel cell electrode polarization including IR components.